The Dynamic Interstellar Medium: A Celebration of the Canadian Galactic Plane Survey
ASP Conference Series, Vol. 438
R. Kothes, T. L. Landecker, and A. G. Willis eds.

The Polarization Signatures of Old Planetary Nebulae in the Canadian Galactic Plane Survey

R. R. Ransom,[1,2] R. Kothes,[2] T. L. Landecker,[2] and M. Wolleben[2]

[1]*Department of Physics and Astronomy, Okanagan College, 583 Duncan Avenue West, Penticton, B.C., V2A 2K8, Canada*

[2]*National Research Council of Canada, Herzberg Institute of Astrophysics, Dominion Radio Astrophysical Observatory, Box 248, Penticton, BC, V2A 6J9, Canada*

Abstract. We present Canadian Galactic Plane Survey (CGPS) polarization images at 1420 MHz centered on two old planetary nebulae (PNe), Sh 2-216 and DeHt 5. Faraday rotation of the diffuse synchrotron background emission in the extended shells of these nebulae is readily observed in the polarization images. In the case of Sh 2-216, we use estimates of electron density and path length to derive the line-of-sight component of the magnetic field in the optically bright north-east portion of the nebula. We interpret our observations via a simple model which describes a deflected and slightly compressed interstellar field around Sh 2-216. In the case of the fast-moving ($\sim$60 km s^{-1}) DeHt 5, we focus on a tail of ionized gas, which starts at the back edge of DeHt 5 and runs away from the nebula in a direction roughly opposite that of the sky-projected space velocity. We believe this tail to be the signature of ionized material ram-pressure stripped first during an interaction between the asymptotic giant branch (AGB) progenitor and the interstellar medium (ISM) and more recently during an interaction between DeHt 5 and the ISM.

1. Introduction

Planetary nebulae (PNe) are expected to interact with the interstellar medium (ISM) when their densities drop below a critical value, and the ram pressure of the ISM begins to dominate the thermal pressure of the expanding nebula (e.g., Borkowski, Sarazin, & Soker 1990). Since the ram pressure is proportional to the square of the speed of the PN system relative to the ambient ISM ($v_{\rm ISM}$), the PN-ISM interaction is expected to start sooner and be more intense for fast-moving systems. These expectations are supported by observations (e.g., Borkowski et al. 1990; Tweedy & Kwitter 1996).

Three-dimensional hydrodynamic simulations have in recent years greatly expanded the picture of the PN-ISM interaction (e.g., Wareing, Zijlstra, & O'Brien 2007). In addition to showing in detail the evolution of the morphology of the PN shell during the interaction, the simulations make two important predictions: (1) material is ram-pressure stripped at the upstream interface between a PN (with $v_{\rm ISM} \gtrsim 25$ km s^{-1}) and the ISM and deposited into a tail behind the system; and (2) the interaction starts before

the PN stage, namely during the later phases of the asymptotic giant branch (AGB) stage. The first of the two predictions is confirmed by the presence of faint tails behind two old PNe, Sh 2-188 and Sh 2-68 (see Xilouris et al. 1996). The second prediction is confirmed by the discovery of a bow shock in front of and a ∼4-pc-long tail behind Mira AB (see Martin et al. 2007).

A good observational tool for the study of the interactions between evolved intermediate-mass stars and the ISM may be radio polarimetric observations. Polarimetric observations at frequencies ≤3 GHz (wavelengths ≥10 cm) are very sensitive to Faraday rotation of the diffuse Galactic synchrotron emission (e.g., Uyanıker et al. 2003). In propagating through the magnetized ISM, the polarized component of the background emission is rotated at wavelength λ [m] through an angle

$$\Delta\theta = RM\,\lambda^2 \text{ [rad]}, \tag{1}$$

where RM is the rotation measure and depends on the line-of-sight component of the magnetic field, $B_\parallel$ [μG], the thermal electron density, n_e [cm^{-3}], and the path length, dl [pc], as

$$RM = 0.81 \int B_\parallel\, n_e\, dl \text{ [rad m}^{-2}\text{]}. \tag{2}$$

Even in the relatively low electron-density environment expected in the tail behind a PN or an AGB star ($n_e \approx n_H \sim 1$ cm^{-3}, see Wareing et al. 2007), a rotation of the background polarization angle of $\Delta\theta > 5°$ can be expected (assuming a 1420 MHz observing frequency and a line-of-sight component of the ISM magnetic field of >2 μG). Such a rotation would result in a Faraday-rotation signature for the tail which is readily observable when contrasted against a smooth off-source region. In the denser and more turbulent interaction region, Faraday rotation of the background emission may be expected to produce highly conspicuous features. In this paper we present the Faraday-rotation signatures of two PNe, Sh 2-216 and DeHt 5, focusing for one (Sh 2-216) on the PN-ISM interaction region and for the other (DeHt 5) on an extended tail-like structure.

2. Properties of Planetary Nebulae Sh 2-216 and DeHt 5

Sh 2-216 and DeHt 5 are old PNe, having estimated kinematic ages of $\gtrsim$200,000 yr and ≈87,000 yr, respectively. Sh 2-216 is the closest known PN at a distance of 129 pc, and is located in the mid-plane of the Galaxy. DeHt 5 is ∼345 pc distant and located at Galactic latitude $b = +11.6°$. The angular diameter of Sh 2-216 is ∼14 times that of DeHt 5 (see Figure 1).

The white dwarf central star (WDCS) in Sh 2-216, LS V 46°21, has a space velocity (corrected for solar motion) of ≈13 km s^{-1}. In contrast, the WDCS in DeHt 5, WD 2218+706, has a space velocity of ≈60 km s^{-1}. The sky-projected space velocities are illustrated in Figure 1. The optical enhancement in the (Galactic) north-east portion of Sh 2-216 denotes a leading-edge interaction between the moving PN and the ISM. In the case of the fast-moving DeHt 5, the bright optical filaments in the northern portion of the shell may coincide with a density enhancement which has moved downstream from the leading edge (see Wareing et al. 2007).

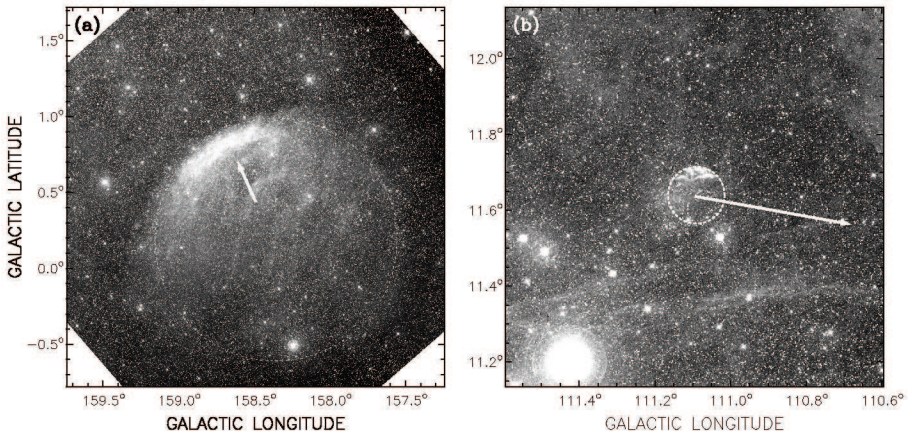

Figure 1. R-band (λ = 657 nm) Digitized Sky Survey images of (*a*) the 2.5° × 2.5° region around Sh 2-216 and (*b*) the 1° × 1° region around DeHt 5. The images are centered on the position of the WDCS, namely LS V 46°21 in (*a*) and WD 2218+706 in (*b*). The gray scale in each image has been adjusted to highlight extended emission, with lighter shades indicating higher intensities. The dashed circle in each image shows the approximate visible extent of the PN. The solid arrow in each image indicates the projected space velocity of the WDCS. The length of each arrow represents the change in sky position for that WDCS over the next ≈50,000 yrs. The angular resolution in each image is ∼1 arcsec.

3. Radio Polarization Images of Sh 2-216 and DeHt 5

In Figure 2 we show the polarized intensity and polarization angle images at 1420 MHz (λ = 21 cm) for a 2.5° × 2.5° region about Sh 2-216. In Figure 3 we show the polarized intensity and polarization angle images at 1420 MHz for a 5° × 5° region about DeHt 5. The images are taken from the Canadian Galactic Plane Survey (CGPS; see Taylor et al. 2003). A detailed description of the preparation of the radio polarization images for the CGPS is given in Landecker et al. (2000).

Figure 2*a* reveals two arc-like structures with low polarized intensity which trace approximately the north-east and north-west edges of the visible disk of Sh 2-216 and low-polarized-intensity "bands" which run approximately east-west across the southern portion of the region. The reduced intensity of these structures, compared to the bright emission north of Sh 2-216, indicates that their appearances are due to the depolarization effects of Faraday rotation (e.g., Gray et al. 1999). The north-east arc is coincident with the optically-identified interaction region at the leading edge of Sh 2-216 (see Figure 1*a*), and almost certainly has an origin in the shell of the PN. The close trace of the north-west arc along the edge of the visible disk of Sh 2-216 suggests that this structure also has an origin in the shell of the PN. The bands are not associated with Sh 2-216.

Figure 3*a* reveals narrow low-polarized-intensity structures on the visible disk of DeHt 5 and a ∼0.5°-long low-polarized-intensity structure which starts at the north-east edge of the disk and runs away from DeHt 5 along a direction approximately opposite that of its projected space velocity. We refer to this elongated structure as the "thick tail," but defer discussion of its possible association with DeHt 5 until Sect. 4.2. If we track north-east from the easternmost edge of the thick tail, we find three additional,

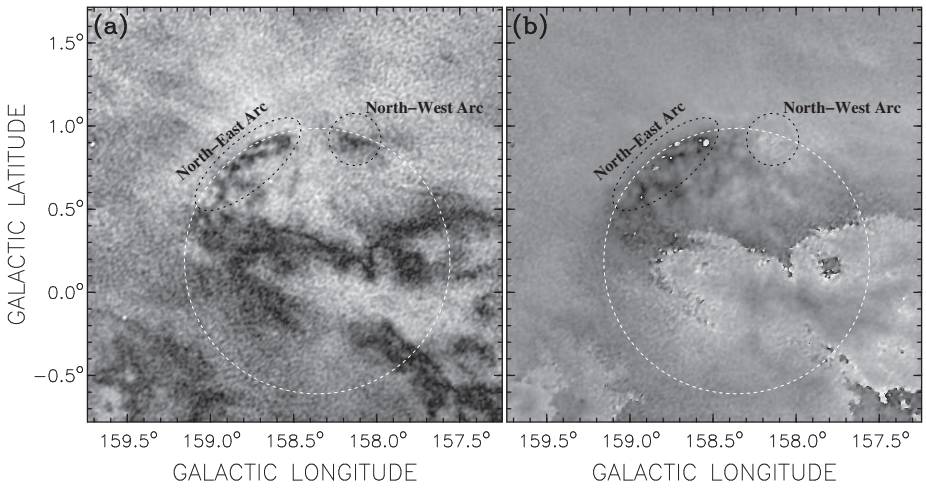

Figure 2. Images at 1420 MHz in (*a*) polarized intensity and (*b*) polarization angle for a 2.5° × 2.5° region around Sh 2-216. Note that the region presented here is identical to that presented in the optical image for Sh 2-216 (Fig 1*a*). The gray scale is in brightness temperature in (*a*), with lighter shades indicating higher temperature. The gray scale in (*b*) extends from −90° (black) to +90° (white). Note that abrupt black-to-white changes in (*b*) do not represent large changes in angle, since polarization angles of −90° and +90° are equivalent. The resolution in each image is ∼1 arcmin. The Faraday-rotation structures on the visible disk of Sh 2-216 (see Sect. 3) are labeled.

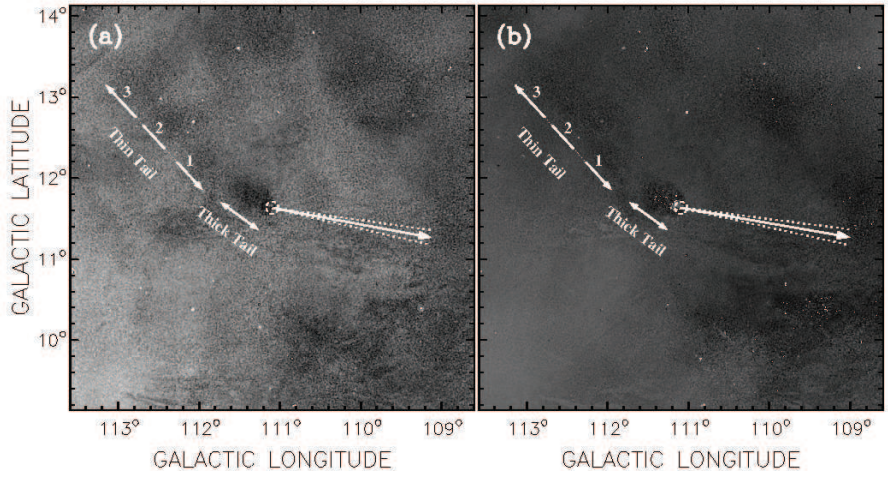

Figure 3. Images at 1420 MHz in (*a*) polarized intensity and (*b*) polarization angle for a 5° × 5° region around DeHt 5. The gray scales and resolution for each image are as described in Fig. 2. The approximate extents of the thick and thin tails described in Sect. 3 are indicated. The three regions comprising the thin tail are labeled 1–3, with the numbers increasing with distance from DeHt 5. The solid arrow and adjacent dotted lines indicate the projected space velocity and space-velocity error cone of WD 2218+706. The length of the arrow represents (at this scale) the change in sky position of WD 2218+706 over the next ≈250,000 yrs.

though more subtle, low-polarized-intensity structures along roughly the same line. We refer collectively to these structures as the "thin tail," and discuss their connection with DeHt 5 in Sect. 4.2. The thick and thin tails, as well as the structures on the disk of DeHt 5, each arise from the depolarization effects of Faraday rotation. We focus below on the thick and thin tails. See Ransom et al. (2010) for a discussion, including close-up view, of the on-disk features.

3.1. Rotation Measures in the Sh 2-216 North-East and North-West Arcs

The polarization angles in the north-east arc are significantly rotated compared to those in the off-source region north of Sh 2-216 (see Figure 2*b*). The largest rotations occur at the centers of several "knots" (regions with white or near-white pixels) within the arc: compare $78^\circ \pm 22^\circ$ for the mean polarization angle in the knots to $7^\circ \pm 6^\circ$ for the mean polarization angle in the off-source region. If we assume that emission with polarization angle $7^\circ \pm 6^\circ$ is incident on the far side of each knot,[1] then the incident emission is Faraday rotated in the knots by $\Delta\theta = -109^\circ \pm 24^\circ$. We infer negative (i.e., clockwise) rotation by tracing the polarization angles from outside the edge of the arc to the center of any knot. For a wavelength of 21 cm, a rotation of $-109^\circ \pm 24^\circ$ gives (via eq. [1]) $RM = -43 \pm 10$ rad m^{-2}.

The polarization angles in the north-west arc are also rotated compared to those in the off-source region (see Figure 2*b*). We were not able to compute the *RM* in the north-west arc, but infer, in the absence of sharp polarization-angle boundaries, a positive (i.e., counter-clockwise) sense of rotation.

3.2. Rotation Measures in the DeHt 5 Thick and Thin Tails

The polarization angles in the thick tail are rotated compared to the immediate off-source region (see Figure 3*b*): compare $-66^\circ \pm 6^\circ$ for the mean polarization angle in the thick tail to $-48^\circ \pm 6^\circ$ for the mean polarization angle in the off-source region. Since the foreground polarized emission is not negligible toward DeHt 5, we used the approach of Wolleben & Reich (2004) to model the Faraday rotation through the thick tail. Our model fits yield a mean *RM* for the thick tail of -15 ± 5 rad m^{-2}. We note that our best-fit model also gives a foreground polarized intensity consistent with that predicted for the ∼345 pc line of sight toward DeHt 5 (see Roger et al. 1999).

The mean polarization angle across all three components of the thin tail is $-55^\circ \pm 6^\circ$, a very modest rotation relative to the $-48^\circ \pm 6^\circ$ off-source region (see Figure 2*b*). If we use the foreground polarized intensity and polarization angle found for the thick tail, we find a mean *RM* for the thin tail of ≈ -7 rad m^{-2}.

---

[1]The off-source polarized emission contains emission from behind Sh 2-216 and emission from between Sh 2-216 and Earth. Since the 129-pc foreground accounts for only ∼10% of the off-source polarized emission (e.g., Beuermann et al. 1985), it is reasonable to assume that the off-source polarization angle is set largely by the background.

4. Discussion

4.1. Magnetic Field in the Shell of Sh 2-216

The interaction region between Sh 2-216 and the ISM is seen clearly in both the R-band optical image (Figure 1*a*) and the radio polarization images (Figure 2). This result is perhaps not surprising considering that ionized material is stacking up in this region, and free electrons contribute to both enhanced optical emission and Faraday rotation. For Faraday rotation, however, an additional ingredient is necessary: a magnetic field. Since we computed the *RM* through polarization-angle knots in the interaction region, we can derive (via eq. [2]) the localized line-of-sight component of the magnetic field in the shell of Sh 2-216. Using $RM = -43 \pm 10$ rad m^{-2}, as well as estimates of the electron density ($n_e = 9.7 \pm 2.3$ cm^{-3}) and path length through the shell ($\Delta l = 1.1 \pm 0.3$ pc) at the positions of the knots (see Ransom et al. 2008), we find a line-of-sight magnetic field of $B_{\|} = 5.0 \pm 2.0\ \mu$G. Since the *RM* is negative, this field is directed into the sky.

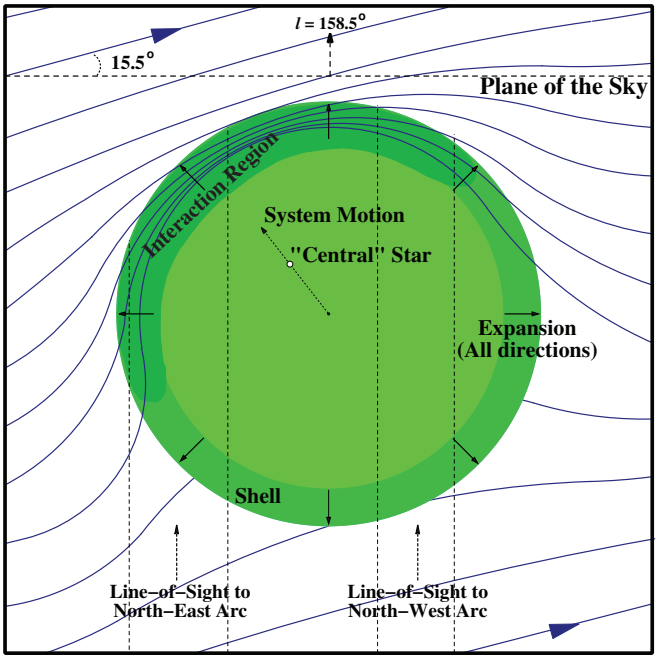

Figure 4. Qualitative model showing the interaction between Sh 2-216 and the magnetized ISM. The perspective is that of an observer sitting above the Galactic plane and looking down on the center of Sh 2-216. The PN is expanding in all directions. The motion of the PN system projected onto the Galactic plane is indicated. LS V 46°21 ("Central" Star) is offset from the center of Sh 2-216 toward the interaction region, where the ISM magnetic field (solid lines) is compressed and deflected around the shell of the PN. The lines-of-sight for an Earthbound observer to the north-east and north-west arcs are indicated. See Ransom et al. (2008) for additional details.

The magnetic field we derive at the position of the knots can be either internal to the PN, i.e., a field originating in LS V 46 or its progenitor, or an ISM field which has diffused part way into the shell. Given the size of Sh 2-216 (diameter $\approx$ 3.8 pc),

an internal field with magnitude $\gtrsim$1 μG seems unlikely, though localized enhancements are possible. On the other hand, an ISM field, which is mildly compressed and deflected at the leading edge of Sh 2-216, can simultaneously explain the into-the-sky field in the interaction region and the out-of-the-sky field (positive *RM*) in the north-west arc. An illustration of this model is presented in Figure 4.

4.2. Evidence Behind DeHt 5 for PN-ISM and AGB-ISM Tails

The best evidence for the thick tail being the Faraday-rotation signature of a PN-ISM tail is its east side attachment to DeHt 5 and the fact that its major axis is approximately aligned with the projected space velocity of WD 2218+706. It is very unlikely that a line-of-sight Faraday-rotation structure, unrelated to DeHt 5, would have this position and alignment. (We address the small, but significant, difference between the position angles of the thick tail and projected space velocity of WD 2218+706 in Ransom et al. 2010.) Also, at a distance of ~345 pc, the projected physical length of the tail is ~3 pc. This tail length corresponds to an interaction age of >74,000 yrs (see Ransom et al. 2010), consistent with the kinematic age of the PN. We present for illustrative purposes a qualitative model showing the interaction between DeHt 5 and the ISM in Figure 5.

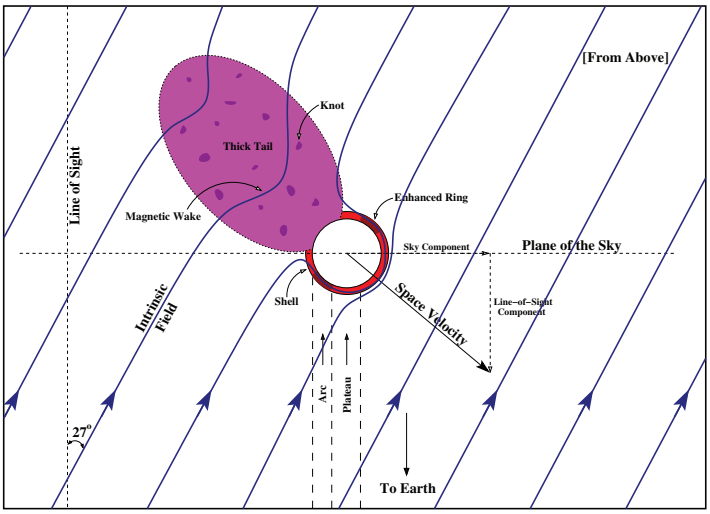

Figure 5. Qualitative model showing the interaction between DeHt 5 and the magnetized ISM. The perspective is that of an observer sitting above the Galactic plane and looking down on DeHt 5. The space velocity of WD 2218+706 is indicated, with line-of-sight and sky components. The field lines immediately surrounding DeHt 5 are compressed and deflected around the leading edge of the shell of the PN. The ~3-pc-long Thick Tail, representing ionized material stripped at the interface between DeHt 5 and the ISM during the PN phase, deflects the intrinsic field in the direction of motion (Magnetic Wake), but not to the same extent as the dense PN shell. See Ransom et al. (2010) for additional details.

If we accept that the thick tail is the signature of the PN-ISM interaction for DeHt 5, then the best evidence that the thin tail is the signature of the earlier AGB-ISM interaction is its relative position behind, and approximate alignment with, the thick tail. The multi-component structure of the thin tail, though qualitatively dissimilar to the more continuous AGB-ISM tail produced in simulations (e.g., Wareing et al. 2007),

may be the product of the last 2–3 thermal-pulse cycles in the DeHt 5 progenitor. The ~11 pc projected length of the thin tail corresponds to an interaction age of >0.23 Myr.

Simulations suggest that a large fraction ($\gtrsim$60%) of the material originally in the envelope of an intermediate-mass star ends up in its tails (Villaver et al. 2003; Wareing et al. 2007). Using our *RM* estimates (see Sect. 3.2) as well as estimates for the line-of-sight magnetic field ($B_{\parallel} = 3.7 \pm 1.3$ μG, see Ransom et al. 2010) and path length ($\Delta l_{\rm av} \approx 1.4$ pc, $\Delta l_{\rm av} \approx 1.2$ pc), we derive ionized masses of 0.7 ± 0.3 $M_{\odot}$ and ~0.5 $M_{\odot}$ for the thick and thin tails, respectively. These estimates include also the ambient ISM mass, but nevertheless indicate that perhaps ~1 $M_{\odot}$ of material has been lost from the system during the interactions. Future radio polarimetric observations of other old PNe and late-stage AGB stars could provide additional insight.

References

Beuermann, K., Kanbach, G., & Berkhuijsen, E. M. 1985, A&A, 153, 17
Borkowski, K. J., Sarazin, C. L., & Soker, N. 1990, ApJ, 360, 173
Gray, A. D., Landecker, T. L., Dewdney, P. E., Taylor, A. R., Willis, A. G., & Normandeau, M. 1999, ApJ, 514, 221
Landecker, T. L., et al. 2000, A&AS, 145, 509
Martin, D. C., et al. 2007, Nat, 448, 780
Ransom, R. R., Kothes, R., Wolleben, M., & Landecker, T. L. 2010, ApJ, 724, 946
Ransom, R. R., Uyaniker, B., Kothes, R., & Landecker, T. L. 2008, ApJ, 684, 1009
Roger, R. S., Costain, C. H., Landecker, T. L., & Swerdlyk, C. M. 1999, A&AS, 137, 7
Taylor, A. R., et al. 2003, AJ, 125, 3145
Tweedy, R. W., & Kwitter, K. B. 1996, ApJS, 107, 255
Uyanıker, B., Landecker, T. L., Gray, A. D., & Kothes, R. 2003, ApJ, 585, 785
Villaver, E., García-Segura, G., & Manchado, A. 2003, ApJ, 585, L49
Wareing, C. J., Zijlstra, A. A., & O'Brien, T. J. 2007, MNRAS, 382, 1233
Wolleben, M., & Reich, W. 2004, A&A, 427, 537
Xilouris, K. M., Papamastorakis, J., Paleologou, E., & Terzian, Y. 1996, A&A, 310, 603